



## Regular Article

# Identification of aqueous access residues of the sodium half channel in transmembrane helix 5 of the $F_0$ - $a$ subunit of *Propionigenium modestum* ATP synthase

Noriyo Mitome<sup>1</sup>, Hiroki Sato<sup>2</sup>, Taishi Tomiyama<sup>1</sup>, Katsuya Shimabukuro<sup>1</sup>, Takuya Matsunishi<sup>1</sup>, Kohei Hamada<sup>1</sup> and Toshiharu Suzuki<sup>3</sup>

<sup>1</sup>Department Chemical and Biological Engineering, National Institute of Technology, Ube College, Ube, Yamaguchi 755-8555, Japan

<sup>2</sup>Chemical Resources Laboratory, Tokyo Institute of Technology, Yokohama, Kanagawa 226-8503, Japan

<sup>3</sup>Department of Applied Chemistry, Graduate School of Engineering, The University of Tokyo, Bunkyo-ku, Tokyo 113-8656, Japan

Received October 18, 2016; accepted February 11, 2017

The  $F_0$ - $a$  subunit of the  $\text{Na}^+$ -transporting  $F_0F_1$  ATP synthase from *Propionigenium modestum* plays a key role in  $\text{Na}^+$  transport. It forms half channels that allow  $\text{Na}^+$  to enter and leave the buried carboxyl group on  $F_0$ - $c$  subunits. The essential Arg residue R226, which faces the carboxyl group of  $F_0$ - $c$  subunits in the middle of transmembrane helix 5 of the  $F_0$ - $a$  subunit, separates the cytoplasmic side and periplasmic half-channels. To elucidate contributions of other amino acid residues of transmembrane helix 5 using hybrid  $F_0F_1$  ( $F_0$  from *P. modestum* and  $F_1$  from thermophilic *Bacillus* PS3), 25 residues were individually mutated to Cys, and effects of modification with the SH-modifying agent N-ethylmaleimide (NEM) on ATP synthesis and hydrolysis activity were analyzed.

Abbreviations: ACMA, 9-amino-6-chloro-2-methoxyacridine; AP5A,  $\text{P}^1, \text{P}^5$ -di(adenosine-5') pentaphosphate; BSA, bovine serum albumin; DDM, n-dodecyl- $\beta$ -D-maltoside; FCCP, carbonyl cyanide *p*-trifluoromethoxyphenylhydrazone; NEM, N-ethylmaleimide; PBS-T, phosphate-buffered saline with Tween-20; SDS-PAGE, sodium dodecyl sulfate polyacrylamide gel electrophoresis; TMH, transmembrane  $\alpha$ -helix

Corresponding author: Norio Mitome, Department of Chemical and Biological Engineering, Ube National College of Technology, Tokiwadai 2-14-1, Ube 755-8555, Japan. e-mail: nmitome@ube-k.ac.jp

NEM significantly inhibited ATP synthesis and hydrolysis as well as proton pumping activities of A214C, G215C, A218C, I223C (cytoplasmic side from R226), and N230C (periplasmic side from R226) mutants and inhibited ATP synthesis activity of the K219C mutant (cytoplasmic side from R226). Thus, these residues contribute to the integrity of the  $\text{Na}^+$  half channel, and both half channels are present in the  $F_0$ - $a$  subunit.

**Key words:** ATPase, chemical modification,  $F_0F_1$ -ATP synthase, ion transport, sodium channel

$F_0F_1$ -ATP synthase ( $F_0F_1$ ) is an enzyme located in the inner mitochondrial membrane, chloroplast thylakoid membrane, and bacterial plasma membrane; it synthesizes or hydrolyzes ATP coupled with  $\text{H}^+$  or  $\text{Na}^+$  transportation [1,2]. The bacterial  $F_0F_1$  has the simplest subunit structure and consists of soluble  $F_1$  with a subunit stoichiometry of  $\alpha_3\beta_3\gamma\delta\epsilon$ , which catalyzes ATP synthesis/hydrolysis, and membrane-integrated  $F_0$  ( $ab_2c_{8-15}$ ), which transports  $\text{H}^+$  across the membrane. In  $F_0$ , the  $c$ -subunit comprises two transmembrane helices connected by a short loop [3] and assembles as an

### ◀ Significance ▶

The  $F_0$ - $a$  subunit of the  $\text{Na}^+$ -transporting  $F_0F_1$  ATP synthase from *Propionigenium modestum* has an important role in  $\text{Na}^+$  transport. To clarify the role of amino-acid residues of transmembrane helix 5 in this subunit, 25 residues were individually mutated to Cys and effects of SH-modification with N-ethylmaleimide (NEM) on ATP synthesis and hydrolysis activity were analyzed. ATP synthesis and hydrolysis and proton pumping activities of A214C, G215C, A218C, I223C and N230C mutants and ATP synthesis activity of the K219C mutant were inhibited. Thus, these residues contribute to the  $\text{Na}^+$  half-channel integrity; both half channels are present in the  $F_0$ - $a$  subunit.

oligomer into a ring structure (*c*-ring), with different number of *c*-subunits depending on the species [4–9]  $F_0F_1$  is a rotary molecular motor [10,11] with a rotor consisting of a  $\gamma\epsilon$ -ring [12] and a stator consisting of  $\alpha_3\beta_3\delta ab_2$ . In  $F_0$ ,  $H^+$  flow drives *c*-ring rotation against  $ab_2$ . In  $F_1$ ,  $\gamma\epsilon$  then rotates against  $\alpha_3\beta_3$ , causing ATP synthesis from ADP and phosphoric acid in the  $\beta$ -subunit. In the reverse reaction, rotation of  $\gamma\epsilon$  in  $F_1$  is driven by ATP hydrolysis. Finally, the *c*-ring in  $F_0$  rotates, and  $H^+$  is transported via a *c*-ring and *a*-subunit.

The *a*-subunit is a highly hydrophobic protein comprising six transmembrane  $\alpha$ -helices in a recently determined structure, whereas it had previously been considered to have five helices. The two long TMHs, corresponding to the TMH5/TMH6 interface of the *a*-subunit [13–16], interact with the *c*-subunit. Moreover, TMH5 contains the conserved Arg residue, known to be essential for proton translocation through the membrane domain of the enzyme; this residue is near another essential Glu residue, in the *c*-subunit. The *a*-subunit contains essential Arg residues (R210 in *E. coli*, R169 in thermophilic *Bacillus* PS3) conserved in  $F_0F_1$  of all species at the boundary of *a*- and *c*-subunits. These residues are assumed to function in  $H^+$  delivery from the *a*-subunit to acidic residues of the *c*-subunit (D61 in *E. coli*, E56 in thermophilic *Bacillus* PS3) located in the middle of the membrane and to couple  $H^+$  flow with *c*-ring rotation [17,18].

While the  $F_0F_1$ -ATP synthase from many species uses an electrochemical potential gradient of  $H^+$  as a driving force for ATP synthesis, enzymes from the obligate anaerobic bacteria *Ilyobacter tartaricus* and *P. modestum* are driven by a  $Na^+$  electrochemical potential gradient [19]. These driving forces for ATP synthesis, i.e., the  $Na^+$  and  $H^+$  electrochemical potential gradients, will be referred to hereafter as  $Na^+$ -transporting and  $H^+$ -transporting types, respectively.

The ion channel  $F_0$  is assumed to be composed of acidic residues located in the middle of the membrane for the *c*-subunit and two half channels opening into the cytoplasmic and periplasmic sides. In the  $H^+$ -transporting-type  $F_0F_1$  of *E. coli*, both cytoplasm-side and periplasm-side half channels have been reported in the *a*-subunit [20]. Amino acid residues forming  $H^+$  half channels have been investigated by introducing a Cys residue into the *a*-subunit was labeled with N-ethylmaleimide (NEM) or  $Ag^+$  [21–24]. The double bond of maleimide in NEM reacts with the thiol group of Cys to form a stable carbon-sulfur bond; this process is irreversible and is expected to occur preferentially in an aqueous environment [25,26].

On the other hand, for the  $Na^+$ -transporting-type  $F_0F_1$ , the periplasmic-side  $Na^+$  half channel is thought to be located in the *a*-subunit since mutations introduced into the periplasmic side of the *a*-subunit abolish  $Na^+$  transfer between the *a*-subunit and *c*-subunit [27], and the cytoplasmic-side  $Na^+$  half channel is located in the *c*-subunit since exogenous  $Na^+$  can bind to the isolated *c*-ring [6]. However, since no  $Na^+$  half channel has been found in the three-dimensional structure of the *c*-ring of another  $Na^+$ -transporting-type  $F_0F_1$  from

*I. tartaricus* [28], the location of the cytoplasmic-side  $Na^+$  half channel is still not clear.

Here, we sought to further elucidate the structure and arrangement of the  $Na^+$ -transporting-type  $F_0F_1$  channel using a system for expressing hybrid  $F_0F_1$  ( $F_0$  from *P. modestum* and  $F_1$  from *Bacillus* PS3) in *E. coli* [29] by analyzing effects of Cys residue chemical modification with the SH-modifying agent NEM on ATP synthesis and hydrolysis activity using inverted membrane vesicles. We hypothesized that cytoplasmic and periplasmic sides of  $Na^+$  half channels in the  $Na^+$ -transporting-type  $F_0F_1$  would be located in the *a*-subunit, similar to the  $H^+$  half channel.

## Materials and Methods

### Construction of a plasmid containing a Cys-mutant

We prepared primers to replace individual amino acid residues between I211 and V236 (except for R226) of the *P. modestum* *a*-subunit with Cys residues (Invitrogen, Carlsbad, CA, USA). The Cys mutant was prepared by the Mega Primer method using the wild-type expression plasmid for hybrid  $F_0F_1$  ( $F_0$  from *P. modestum*, and  $F_1$  from *Bacillus* PS3 [pTR-*hF\_1F\_0*<sup>(-i)</sup>]) as a template [29]. For Ni-NTA purification of  $F_0F_1$ , His-tag residues (10) were conjugated to the N-terminus of the  $\beta$  subunit. The nucleotide sequence of each Cys mutant was verified with a DNA sequencer.

### Preparation of inverted membranes containing wild-type and Cys-mutant proteins and confirmation of protein expression

The Cys-mutant plasmid was transformed into  $F_0F_1$ -deficient *E. coli* JM103  $\Delta(uncB-uncD)$  with plasmid PST-I [29]. To culture the transformants, preparation of membrane vesicles were performed as previously described [29]. Membrane vesicles were analyzed by 0.1% SDS–15% PAGE. Proteins were visualized with Coomassie brilliant blue R.  $F_0F_1$  expression was confirmed by immunoblotting analysis using an anti- $\beta$  polyclonal antibody for the  $TF_1$ . Purified  $F_0F_1$  enzyme with a defined concentration was used as a standard; band quantification was performed using Sonic Image software.

### ATP synthesis activity assay

ATP synthesis activity was measured at 35°C using luciferase assays as previously described [29]. Inverted membranes at 5 mg/mL were incubated with 5 mM NEM for 15 min at room temperature. Then, 1.6 mL PA3- $NO_3$  buffer (10 mM HEPES-KOH [pH 7.5], 10% glycerol, 5 mM  $Mg(NO_3)_2$ , 2.5 mM KPi (pH 7.5), 0.53 mM ADP (Calbiochem, San Diego, CA, USA), 26.6  $\mu$ M  $P^i, P^s$ -di(adenosine-5') pentaphosphate (AP5A; Sigma, St. Louis, MO, USA), 20  $\mu$ L the inverted membrane, 0.125 volumes of CLS II solution (ATP Bioluminescence Assay Kit CLS II; Roche), 2.5 mM NaCl, and 3.125  $\mu$ M monensin (Calbiochem) were added into a cuvette. After the measurement was started,

0.5 mM NADH was added. The amounts of ATP synthesized were calibrated with a defined amount of ATP at the end of the measurement.

Specific activity was calculated based on three parameters, including estimated F<sub>0</sub>F<sub>1</sub> concentration, the slope of ATP synthesis activity measured for 50 s immediately after NADH addition (excluding the slope of data recorded 100 s immediately before NADH addition), and the ATP calibration value.

#### ATP hydrolysis activity assay

ATP hydrolysis activity was measured with an ATP-regenerating system at 30°C [17]. Inverted membranes at 5 mg/mL were incubated with 5 mM NEM for 15 min at room temperature. Then, 1.5 mL PA3 Buffer (10 mM HEPES-KOH [pH 7.5], 10% glycerol, 5 mM MgCl<sub>2</sub>), 50 mM Tris (pH 7.5), 100 mM KCl, 2.5 mM PEP, 5.0 mM MgCl<sub>2</sub>, 2.0 mM ATP, 10 µg/mL pyruvate kinase, 10 µg/mL lactic dehydrogenase, 2 mM NADH, 2.5 mM KCN, and 0.1 µg/mL carbonyl cyanide *p*-trifluoromethoxyphenylhydrazone (FCCP) were added into each cell. A 20-µL sample of the inverted membrane preparation was added at 30 s after starting the measurement, and the slope was measured over 300 s. The specific activity and inhibition rate were calculated using the protein assay-based protein concentration and the slope of 240–300 s data in the ATPase activity assay.

#### Proton-pumping activity

ATPase-driven H<sup>+</sup>-pumping activity was assayed with fluorescence quenching of 9-amino-6-chloro-2-methoxy-acridine (ACMA; excitation at 410 nm, emission at 480 nm) at 37°C as described previously [29]. Inverted membranes at 5 mg/mL were incubated with 5 mM NEM for 15 min at room temperature. Inverted membrane vesicles were added to the assay mixture at a final concentration of 0.2 mg membrane protein/mL. The reaction was initiated by adding 1 mM K<sup>+</sup>-ATP and terminated with 0.25 µg/mL FCCP. The level of fluorescence obtained after the addition of FCCP was normalized to 100% in calculating the percentage of quenching due to ATP-driven proton pumping.

## Results

### Preparation of the inverted membranes of wild-type and Cys-mutant proteins and confirmation of expression levels

The inverted membranes were prepared from *E. coli* expressing F<sub>0</sub>F<sub>1</sub>-ATP synthase mutants. Setting R226 as the center, the cytoplasmic side was defined as residues between I211C and I225C, and the periplasmic side was defined as those between L227 and V236. Expression of F<sub>0</sub>F<sub>1</sub> in wild-type and Cys-mutant preparations was confirmed by SDS-PAGE. The expression levels of the Cys-mutant F<sub>0</sub>F<sub>1</sub> enzymes varied from 10% of total membrane protein in low-expression mutants to 30% in wild-type and high-

expression mutants in each membrane. Nevertheless, these results confirmed that all mutant F<sub>0</sub>F<sub>1</sub> proteins were expressed in the membrane preparations.

### ATP synthesis activity of wild-type and Cys-mutant enzymes

Addition of NADH to inverted membranes generates an electrochemical potential gradient of H<sup>+</sup> because of H<sup>+</sup> pumping to the membrane interior by the membrane respiratory chain. The Na<sup>+</sup>/H<sup>+</sup> antiporter monensin converts some amount of the H<sup>+</sup> electrochemical potential gradient into a Na<sup>+</sup> electrochemical potential gradient across the membrane, which is utilized by F<sub>0</sub>F<sub>1</sub> for synthesis of ATP from ADP and phosphoric acid. Therefore, we investigated changes in ATP synthesis activity of inverted membrane preparations of wild-type and Cys-mutant enzymes upon chemical modification of Cys residues with NEM.

In the presence of FCCP, an H<sup>+</sup>-decoupling agent that binds to membranes and eliminates the H<sup>+</sup> concentration difference between the inside and outside of the membrane, no increase in luminescence detected at 560 nm was observed upon addition of NADH, indicating that ATP synthesis did not occur (Supplementary Fig. S1). However, an increase was observed upon addition of NADH, and slopes indicated that ATP was synthesized, both with and without addition of NEM. Thus, once the Na<sup>+</sup> electrochemical potential gradient was neutralized by ATP synthesis, slopes of the curves were lost, and luminescence plateaued. During this phase, ATP calibration was performed. Additionally, for the wild-type enzyme, the slope of the curve immediately after NADH addition was similar, regardless of NEM treatment. Thus, these data suggest that ATP synthesis by the wild-type enzyme is not inhibited by NEM.

Next, we analyzed the ATP synthesis activity for each of the Cys mutants (Supplementary Fig. S1). The specific activity of the wild-type enzyme used in this study was 4.3 mU/mg membrane protein (15 mU/mg F<sub>0</sub>F<sub>1</sub>), which was in agreement with value described in the literature (3.4 mU/mg membrane protein [29]). Concerning specific activities of individual Cys mutants, I211C–L213C mutants showed about 70–80% of the wild-type activity, the A214C mutant showed as much as activity as the wild-type enzyme, G215C–V236C mutants (except for G234C) showed about 10–40% of the wild-type activity, and the G234C mutant showed only 3% of the wild-type activity (Fig. 1A). Results showed that the activity of each mutant (baseline compared to NEM) was statistically significant (t-test; *p* < 0.05). Although the specific activity of G234C was very low, the result confirmed that each mutant had enzyme activity.

### A214, G215, A218, K219, I223, and N230 residues were important for ATP synthesis

As was the case with the wild-type enzyme, the slope of the curve immediately after NADH addition obtained with and without NEM treatment was comparable for most Cys

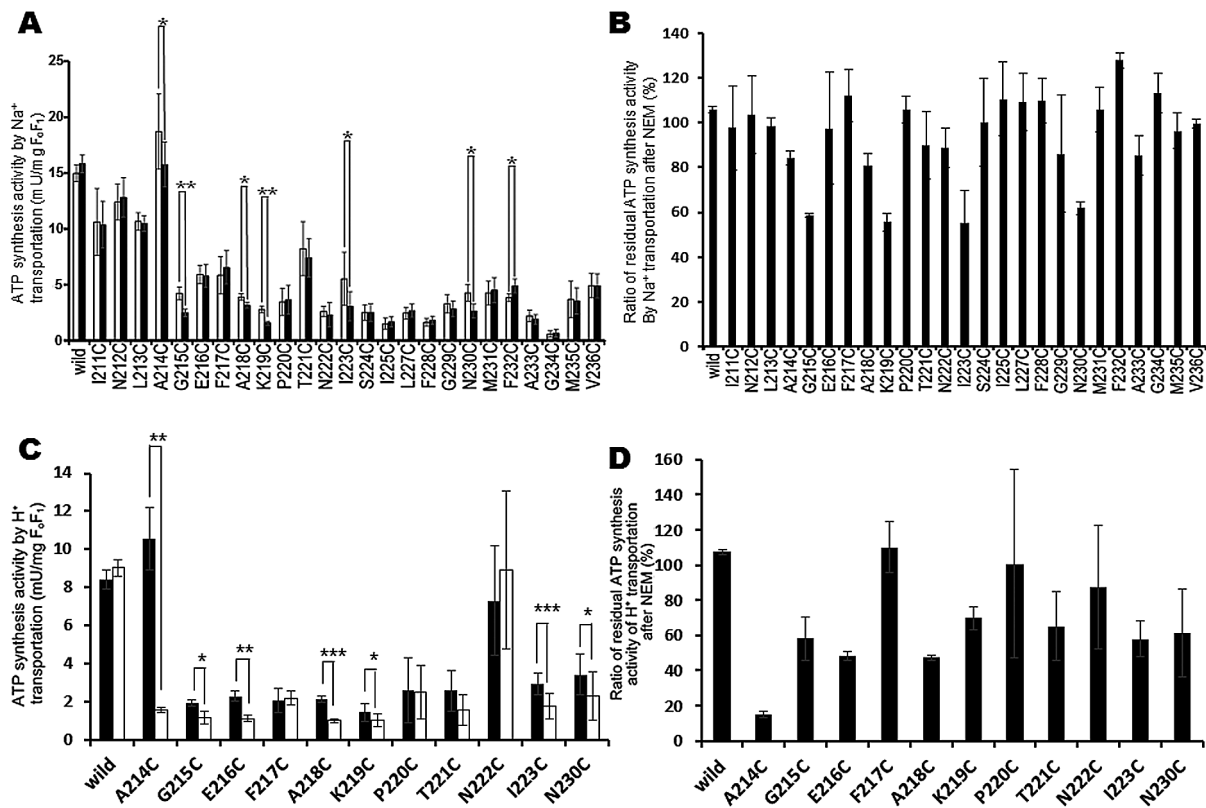


**Figure 1** A: ATP synthesis activities in the presence of monensin for wild-type protein and individual Cys mutants with and without NEM treatment. Results presented are averages of  $\geq 3$  determinations  $\pm$  SDs. B: Percent residual ATP synthesis activity in the presence of monensin of NEM-treated wild-type proteins and Cys mutants, indicating degree of change in ATP synthesis activity between NEM-treated and untreated constructs. Residual activity was determined as the ratio of the specific activity obtained with NEM treatment to that obtained without NEM treatment. Results presented are averages of  $\geq 3$  determinations  $\pm$  SDs. C: ATP synthesis activity in the absence of monensin for Cys-substituted A214-I223 and N230 mutants. D: Percent residual ATP synthesis without monensin of NEM-treated Cys mutants. Results are presented as averages  $\pm$  SDs of triplicate experiments. Statistical analyses of differences between samples with and without NEM treatment were performed using Student's *t* tests. \* $p < 0.05$ , \*\* $p < 0.01$ , \*\*\* $p < 0.001$ .

mutants (data not shown). However, in the cases of A214C, G215C, A218C, K219C, I223C, and N230C mutants, NEM treatment reduced the slope immediately after NADH addition compared to that obtained without NEM treatment; therefore, ATP synthesis by these mutants appear to be inhibited by NEM (Fig. 2 and Supplementary Fig. S1). Moreover, for mutations in the cytoplasmic side, in the presence of NEM, the A214C, G215C, A218C, K219C, and I223C mutations caused  $18 \pm 3.3\%$ ,  $42 \pm 0.9\%$ ,  $19 \pm 5.3\%$ ,  $43 \pm 3.9\%$ , and  $45 \pm 13.7\%$  inhibition of ATP synthesis activity, respectively (Fig. 1B). In contrast, the ATP synthesis activity of N230C, with a mutation in the periplasmic side, was inhibited by  $38 \pm 3.0\%$  upon NEM treatment (Fig. 1B). These residues may represent residues to which NEM is accessible from the outside of the membrane. When Cys substitutions were labeled by NEM, Na<sup>+</sup> was blocked by NEM, and Na<sup>+</sup> transfer from the periplasmic side to the cytoplasmic side was abolished; thus, ATP synthase activity was inhibited.

Since F<sub>0</sub> from *P. modestum* can facilitate coupled transport of protons, inhibition of ATP synthesis by NEM in the absence of monensin in these mutants was an interesting

finding. We examined the effects of NEM on the inhibition of ATP synthesis in Cys mutants of A214-I223 and N230. ATP synthesis activities without monensin were relatively lower than in conditions with monensin. Among these mutants, in the presence of NEM, the A214C, G215C, A218C, K219C, I223C, and N230C mutations caused statistically significant inhibition of ATP synthesis (i.e.,  $84 \pm 1.77\%$ ,  $41 \pm 12.3\%$ ,  $53 \pm 1.2\%$ ,  $30 \pm 6.7\%$ ,  $43 \pm 10.0\%$ , and  $38 \pm 24.9\%$  inhibition, respectively) in the absence of monensin (Fig. 1D). E216C showed  $50 \pm 2.6\%$  inhibition, though this mutant was not inhibited by NEM in the presence of monensin. Taken together, these results suggest that glutamate residues of E216 play an important role in H<sup>+</sup> channels, but are associated with the Na<sup>+</sup> channel.

#### A214, G215, I223, and N230 residues were important for ATP hydrolysis activity

Specific activity calculated based on F<sub>0</sub>F<sub>1</sub> concentration data in each membrane. Although some of the mutants showed low specific activities (0.50 U/mg F<sub>0</sub>F<sub>1</sub> or lower), i.e., G215C, E216C, P220C, and N230C, all mutants had

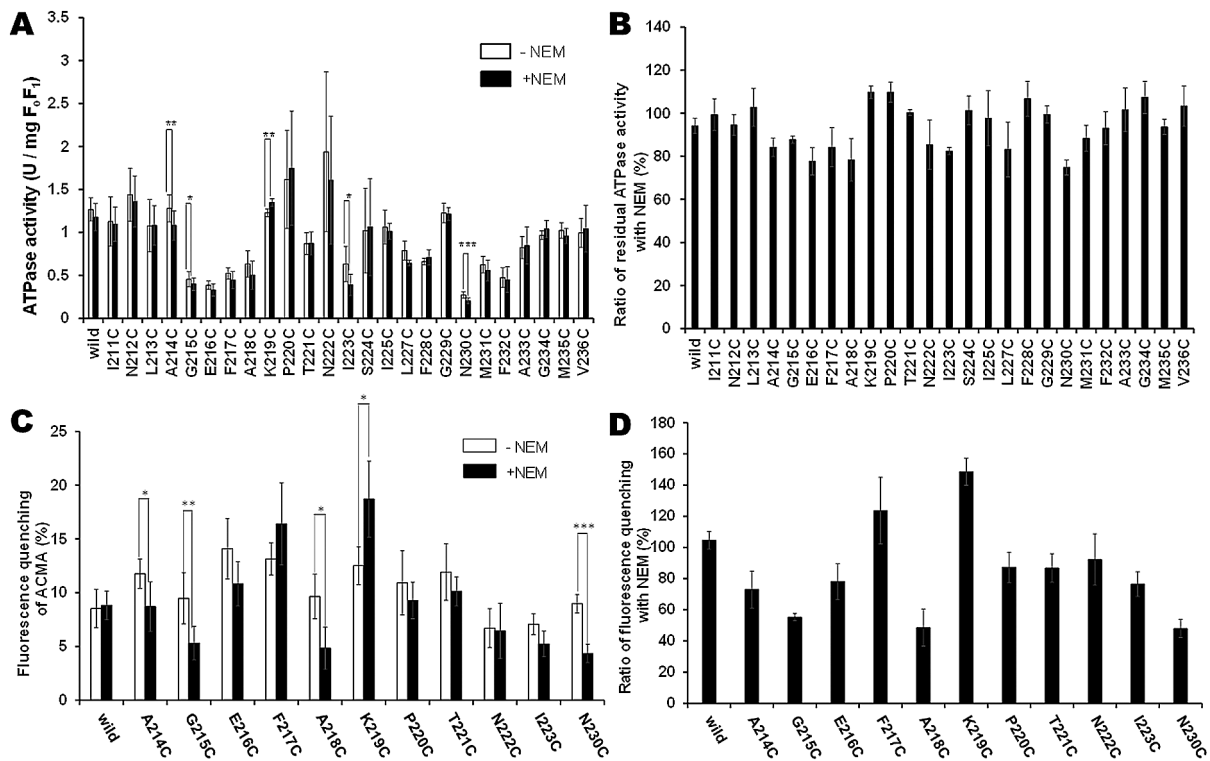


**Figure 2** A: ATPase activity for wild-type proteins and I211C–V236C mutants (except for R226C) with and without NEM treatment. Results presented are averages of  $\geq 3$  determinations  $\pm$  SDs. B: Percent residual ATPase activity of NEM-treated wild-type proteins and Cys mutants, indicating degree of change in ATPase activity between NEM-treated and untreated constructs. Residual activity was determined as the ratio of the specific activity obtained with NEM treatment to that obtained without NEM treatment. Results are presented as means  $\pm$  SDs of triplicate experiments. C: Proton pump-mediated ACMA fluorescence quenching of Cys-substituted A214–I223 and N230 mutants. Maximum extent of quenching induced by addition of ATP is shown. D: Percent residual ACMA fluorescence quenching of NEM-treated Cys mutants. The ratio of ACMA fluorescence quenching obtained with NEM treatment to that obtained without NEM treatment. Results are presented as averages  $\pm$  SDs of triplicate experiments. Statistical analyses of differences between samples with and without NEM treatment were performed using Student's *t* tests. \**p* < 0.05, \*\**p* < 0.01, \*\*\**p* < 0.001.

measurable ATP hydrolysis activity.

Next, we compared data between wild-type protein and Cys mutants I211C–V236C obtained with and without NEM treatment (Fig. 2A). For the wild-type enzyme, the specific activity did not show statistical significance with NEM treatment (Fig. 2B). Concerning mutations in the cytoplasmic side, the A214C, G215C, and I223C mutation caused significant inhibition of ATPase activity by NEM (i.e.,  $16 \pm 4.3\%$ ,  $12 \pm 1.7\%$ , and  $19 \pm 1.2\%$  inhibition, respectively) (Fig. 2B). Moreover, the ATPase activity of N230C, with a mutation in the periplasmic side, was inhibited by  $25 \pm 3.5\%$  upon NEM treatment. Therefore, Cys mutation and NEM modification resulted in inhibition of ATPase activity at these four residues, suggesting that these residues may constitute the Na<sup>+</sup> half channel.

#### A214, G215, A218, and N230 residues were important for ion transport

To analyze ion transport from the cytoplasmic side to the periplasmic side through the F<sub>0</sub> *a*-subunit, the proton pump-mediated ACMA fluorescence quenching of Cys-substituted

mutants was analyzed with and without NEM. The mutants I211C–L213C, S224C, I225C, L227C–G229C, and M231C–V236C either did not exhibit activity or had activity that was too low for detection in the presence or absence of NEM. Mutants A214C–I223C and N230C effectively quenched ACMA fluorescence (Fig. 2C and Supplementary Fig. S2). Among these mutants, A214C, G215C, A218C, and N230C showed significant decrease in the presence of NEM ( $26 \pm 11.8\%$ ,  $44 \pm 2.3\%$ ,  $50 \pm 11.9\%$ , and  $52 \pm 11.9\%$  decrease, respectively) (Fig. 2D). However, K219C showed significant increase with NEM.

## Discussion

### Both cytoplasmic-side and periplasmic-side Na<sup>+</sup> half channels were present in the *a*-subunit

From the results described here, we concluded that A214, G215, A218, K219, I223, and N230 residues of TMH4 of the *a*-subunit contributed to the integrity of the Na<sup>+</sup> half channel, and both the cytoplasmic-side and periplasmic-side half channels were present in the *a*-subunit of the Na<sup>+</sup> transport-

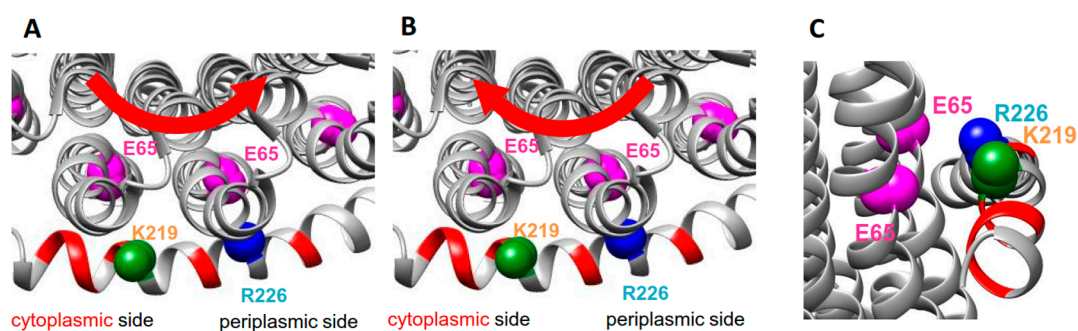


**Figure 3** Position of NEM-sensitive residues in an  $F_0$   $a$ -subunit structural model. A: ATP synthesis. B: ATP hydrolysis. C: Side view. NEM-sensitive residues were colored red (sensitive to ATP synthesis and ATP hydrolysis) or green (only sensitive to ATP synthesis) in the structure of *Paracoccus denitrificans*  $F_0$   $a$ . Indicated numbers are numbers of residues of *Propionigenium modestum*  $F_0$   $F_1$ -ATP synthase, which were equivalent to the position of *Paracoccus denitrificans*  $F_0$   $F_1$ -ATP synthase.

ing  $F_0$   $F_1$  ATP synthase (Fig. 3). The sodium transport mechanism in ATP synthase suggested that a sodium ion entering a  $Na^+$  half-channel via the N230 in  $a$ -subunit was transferred to a carboxyl group within the  $c$ -subunit in the  $c$ -ring, enabling this  $c$ -subunit to move into the lipid-surrounding environment. The  $c$ -ring would then make almost one revolution carrying the  $Na^+$  near the other  $Na^+$  half-channel constituting of A214, G215, A218, K219, I223 in the  $a$ -subunit, where the  $Na^+$  would be transferred. Since the residues A214, G215, A218, and K219 exist close to the  $c$ -ring in the structure of  $F_0$   $F_1$  ATP synthase, the inhibition of the activities of ATP synthase by modification of these residues by NEM occurred not only because these residues consist of ion channels but because NEM of these residues would block the rotation of  $c$ -ring.

#### K219 functioned as a channel in ATP synthesis but not ATP hydrolysis

Concerning differences between the inhibition of ATP synthesis and ATP hydrolysis, the degree of ATP hydrolysis inhibition tended to be lower than that of ATP synthesis inhibition. This may be because the measured ATPase activity partly included the activity derived from the uncoupled enzyme, while the ATP synthesis activity assay detects only the activity coupled with  $Na^+$  ion transport. This may be why NEM modification of G215C, I223C, and N230C diminished ATP synthesis activity more than the ATPase activity. Among the mutants, the K219C mutant showed no reduction in ATPase and proton-pumping activities, but caused a 50% reduction in ATP synthesis activity, suggesting that K219 functioned as a channel in ATP synthesis but not ATP hydrolysis.

#### Differences between the $Na^+$ and $H^+$ half channels

In the case of *E. coli*  $F_0$   $F_1$ -ATP synthase, NEM modifications on the periplasmic side occurred at N214C, consistent with the N230C modification in *P. modestum*. With regard to residues in the cytoplasmic side, while only S206C was modified in *E. coli*, modification of A214, G215, A218,

K219, and I223 was observed in *P. modestum*. Since the corresponding residues in *E. coli* were modified with  $Ag^+$ , the channel-constituting residues were thought to be consistent with those in *E. coli*. Given that NEM modifications were observed in *P. modestum* but not *E. coli*, a space sufficient for NEM to bind is suggested to be available in the channel around G215 and K219 in the  $a$ -subunit of *P. modestum*  $F_0$   $F_1$ -ATP synthase. This suggests that the *P. modestum*  $Na^+$  ion channel is larger than its *E. coli* counterpart in order to accommodate  $Na^+$ , which has a larger ionic radius than  $H^+$ . Nevertheless, additional experiments using  $Ag^+$  will be beneficial, since some NEM-insensitive residues can be sensitive to  $Ag^+$  due to the small size of  $Ag^+$  as compared to the bulky NEM molecule.

#### Conclusion

In summary, we have identified aqueous access residues in TMH5 of the  $a$ -subunit that appear to participate in  $Na^+$  transport in  $F_0$   $F_1$  ATP synthase, suggesting that both the cytoplasmic and periplasmic sides of  $Na^+$  half channels existed in the  $a$ -subunit. The expression system for a hybrid  $F_0$   $F_1$  composed of the  $Na^+$ -transport-type  $F_0$  from *P. modestum* and  $F_1$  from thermophilic *Bacillus* PS3 may help reveal the  $Na^+$  channel structure and facilitate analysis of the  $Na^+$  transport mechanism. The hybrid  $F_0$   $F_1$  presents advantages in the preparation of a stable mutant  $F_0$   $F_1$  complex because  $F_1$  from *Bacillus* PS3 is more stable than  $F_1$  from *P. modestum*. Additional studies, including analysis of residues of other TMHs within the  $a$ -subunit and  $c$ -subunit, crosslink analysis of the two helices of the  $a$ -subunit based on structural analysis of the  $a$ -subunit with the  $c$ -ring will be required to fully elucidate the  $Na^+$  transporting mechanism.

#### Acknowledgments

We thank Drs. M. Yoshida and T. Hisabori for helpful discussions. This work was supported by Japan Society for the Promotion of Science (JSPS) KAKENHI Grant Number

23770160; the Cooperative Research Program of the Network Joint Research Center for Materials and Devices; and the National Institute of Technology, Ube College Special Fund for Education and Research.

## Conflicts of Interest

The authors declare no competing financial interest.

## Author Contribution

N. M directed the entire project and wrote the manuscript. T. S. developed expression system of enzyme and analytical system, directed the project. H. S. prepared mutants and analyzed ATP synthesis activity. T. T. carried out analysis of activity and molecular modeling. K. S. supervised molecular modeling and gave important aspects for revision. T. M and K. H analyzed ATP hydrolysis activity.

## References

- [1] Boyer, P. D. The ATP synthase—a splendid molecular machine. *Annu. Rev. Biochem.* **66**, 717–749 (1997).
- [2] Yoshida, M., Muneyuki, E. & Hisabori, T. ATP synthase—a marvellous rotary engine of the cell. *Nat. Rev. Mol. Cell Biol.* **2**, 669–677 (2001).
- [3] Girvin, M. E., Rastogi, V. K., Abildgaard, F., Markley, J. L. & Fillingame, R. H. Solution structure of the transmembrane H<sup>+</sup>-transporting subunit *c* of the F<sub>1</sub>F<sub>0</sub> ATP synthase. *Biochemistry* **37**, 8817–8824 (1998).
- [4] Stock, D., Leslie, A. G. & Walker, J. E. Molecular architecture of the rotary motor in ATP synthase. *Science* **286**, 1700–1705 (1999).
- [5] Stahlberg, H., Muller, D. J., Suda, K., Fotiadis, D., Engel, A., Meier, T., *et al.* Bacterial Na(+)-ATP synthase has an undecameric rotor. *EMBO Rep.* **2**, 229–233 (2001).
- [6] Meier, T., Matthey, U., von Ballmoos, C., Vonck, J., Krug von Nidda, T., Kühlbrandt, W., *et al.* Evidence for structural integrity in the undecameric *c*-rings isolated from sodium ATP synthases. *J. Mol. Biol.* **325**, 389–397 (2003).
- [7] Seelert, H., Poetsch, A., Dencher, N. A., Engel, A., Stahlberg, H. & Muller, D. J. Structural biology. Proton-powered turbine of a plant motor. *Nature* **405**, 418–419 (2000).
- [8] Jiang, W., Hermolin, J. & Fillingame, R. H. The preferred stoichiometry of *c* subunits in the rotary motor sector of *Escherichia coli* ATP synthase is 10. *Proc. Natl. Acad. Sci. USA* **98**, 4966–4971 (2001).
- [9] Mitome, N., Suzuki, T., Hayashi, S. & Yoshida, M. Thermophilic ATP synthase has a decamer *c*-ring: indication of non-integer 10:3 H<sup>+</sup>/ATP ratio and permissive elastic coupling. *Proc. Natl. Acad. Sci. USA* **101**, 12159–12164 (2004).
- [10] Abrahams, J. P., Leslie, A. G., Lutter, R. & Walker, J. E. Structure at 2.8 Å resolution of F<sub>1</sub>-ATPase from bovine heart mitochondria. *Nature* **370**, 621–628 (1994).
- [11] Noji, H., Yasuda, R., Yoshida, M. & Kinoshita Jr., K. Direct observation of the rotation of F<sub>1</sub>-ATPase. *Nature* **386**, 299–302 (1997).
- [12] Tsunoda, S. P., Aggeler, R., Yoshida, M. & Capaldi, R. A. Rotation of the *c* subunit oligomer in fully functional F<sub>1</sub>F<sub>0</sub> ATP synthase. *Proc. Natl. Acad. Sci. USA* **98**, 898–902 (2001).
- [13] Morales-Rios, E., Montgomery, M. G., Leslie, A. G. & Walker, J. E. Structure of ATP synthase from *Paracoccus denitrificans* determined by X-ray crystallography at 4.0 Å resolution. *Proc. Natl. Acad. Sci. USA* **112**, 13231–13236 (2015).
- [14] Allegretti, M., Klusch, N., Mills, D. J., Vonck, J., Kühlbrandt, W. & Davies, K. M. Horizontal membrane-intrinsic  $\alpha$ -helices in the stator *a*-subunit of an F-type ATP synthase. *Nature* **521**, 237–240 (2015).
- [15] Zhou, A., Rohou, A., Schep, D. G., Bason, J. V., Montgomery, M. G., Walker, J. E., *et al.* Structure and conformational states of the bovine mitochondrial ATP synthase by cryo-EM. *Elife* **4**, e10180 (2015).
- [16] Hahn, A., Parey, K., Bublitz, M., Mills, D. J., Zickermann, V., Vonck, J., *et al.* Structure of a complete ATP synthase dimer reveals the molecular basis of inner mitochondrial membrane morphology. *Mol. Cell* **63**, 445–456 (2016).
- [17] Valiyaveetil, F. I. & Fillingame, R. H. On the role of Arg-210 and Glu-219 of subunit *a* in proton translocation by the *Escherichia coli* F<sub>0</sub>F<sub>1</sub>-ATP synthase. *J. Biol. Chem.* **272**, 32635–32641 (1997).
- [18] Mitome, N., Ono, S., Sato, H., Suzuki, T., Sone, N. & Yoshida, M. Essential arginine residue of the F<sub>0</sub>-*a* subunit in F<sub>0</sub>F<sub>1</sub>-ATP synthase has a role to prevent the proton shortcut without *c*-ring rotation in the F<sub>0</sub> proton channel. *Biochem. J.* **430**, 171–177 (2010).
- [19] Dimroth, P. Primary sodium ion translocating enzymes. *Biochim. Biophys. Acta* **1318**, 11–51 (1997).
- [20] Vik, S. B. & Antonio, B. J. A mechanism of proton translocation by F<sub>1</sub>F<sub>0</sub> ATP synthases suggested by double mutants of the *a* subunit. *J. Biol. Chem.* **269**, 30364–30369 (1994).
- [21] Angevine, C. M., Herold, K. A. & Fillingame, R. H. Aqueous access pathways in subunit *a* of rotary ATP synthase extend to both sides of the membrane. *Proc. Natl. Acad. Sci. USA* **100**, 13179–13183 (2003).
- [22] Angevine, C. M. & Fillingame, R. H. Aqueous access channels in subunit *a* of rotary ATP synthase. *J. Biol. Chem.* **278**, 6066–6074 (2003).
- [23] Angevine, C. M., Herold, K. A., Vincent, O. D. & Fillingame, R. H. Aqueous access pathways in ATP synthase subunit *a*. Reactivity of cysteine substituted into transmembrane helices 1, 3, and 5. *J. Biol. Chem.* **282**, 9001–9007 (2007).
- [24] Moore, K. J., Angevine, C. M., Vincent, O. D., Schwem, B. E. & Fillingame, R. H. The cytoplasmic loops of subunit *a* of *Escherichia coli* ATP synthase may participate in the proton translocating mechanism. *J. Biol. Chem.* **283**, 13044–13052 (2008).
- [25] Kimura-Someya, T., Iwaki, S., Konishi, S., Tamura, N., Kubo, Y. & Yamaguchi, A. Cysteine-scanning mutagenesis around transmembrane segments 1 and 11 and their flanking loop regions of Tn10-encoded metal-Tetracycline/H<sup>+</sup> antiporter. *J. Biol. Chem.* **275**, 18692–18697 (2000).
- [26] Mordoch, S. S., Granot, D., Lebendiker, M. & Schuldiner, S. Scanning cysteine accessibility of EmrE, an H<sup>+</sup>-coupled multi-drug transporter from *Escherichia coli*, reveals a hydrophobic pathway for solutes. *J. Biol. Chem.* **274**, 19480–19486 (1999).
- [27] Kaim, G., Matthey, U. & Dimroth, P. Mode of interaction of the single *a* subunit with the multimeric *c* subunits during the translocation of the coupling ions by F<sub>1</sub>F<sub>0</sub> ATPases. *EMBO J.* **17**, 688–695 (1998).
- [28] Meier, T., Polzer, P., Diederichs, K., Welte, W. & Dimroth, P. Structure of the rotor ring of F-Type Na<sup>+</sup>-ATPase from *Ilyobacter tartaricus*. *Science* **308**, 659–662 (2005).
- [29] Suzuki, T., Ozaki, Y., Sone, N., Feniouk, B. A. & Yoshida, M. The product of *uncl* gene in F<sub>1</sub>F<sub>0</sub>-ATP synthase operon plays a chaperone-like role to assist *c*-ring assembly. *Proc. Natl. Acad. Sci. USA* **104**, 20776–20781 (2007).